

Synthesis, Crystal Structures, and Magnetic Properties of a Mono- and a Dinuclear Copper(II) Complex of the 2,4,6-Tris(2-pyridyl)-1,3,5-triazine Ligand

Thorsten Glaser,^{*,[a]} Thomas Lügger,^[a] and Roland Fröhlich^[b]

Keywords: Magnetic properties / Copper / N ligands / Coordination chemistry

The reaction of 2,4,6-tris(2-pyridyl)-1,3,5-triazine (tptz) with $\text{Cu}(\text{BF}_4)_2 \cdot 3\text{H}_2\text{O}$ and *N,N*-bis(3-aminopropyl)methylamine (Medpt) yielded the monomeric complex $[(\text{tptz})\text{Cu}^{\text{II}}(\text{Medpt})](\text{BF}_4)_2 \cdot 2\text{MeOH}$ (**1**) whereas reaction of tptz with $\text{CuCl}_2 \cdot 2\text{H}_2\text{O}$ yielded the dinuclear complex $[(\text{Cu}^{\text{II}}\text{Cl}_2)(\text{tptz})\{\text{Cu}^{\text{II}}\text{Cl}_2(\text{MeOH})\}]$ (**2**). The molecular structures of **1** and **2** were established by single-crystal X-ray diffraction studies. The copper ion in complex **1** is elongated octahedral with the nitrogen atoms of Medpt and the triazine nitrogen atom of tptz in the equatorial positions, and the two pyridyl nitrogen atoms of tptz in axial positions. The two Cu^{II} ions in complex **2** are bridged by tptz, coordinating to Cu1 in a terpyridine-like fashion and to Cu2 in a bipyridine-like coordination mode. The triazine nitrogen atom bound to Cu1 is coordinated in an equatorial position whereas the triazine nitrogen atom bound to Cu2 is situated in the apical position. The equatorial plane of Cu1 is coplanar with the 1,3,5-triaz-

ine plane whereas the equatorial plane of Cu2 is perpendicular to the 1,3,5-triazine plane. Intermolecular interactions in the solid state result in both compounds in "dimeric units" due to hydrogen bonding. Both complexes were investigated by variable-temperature magnetic susceptibility measurements. Through-space dipolar couplings and/or weak through-bond interactions in complex **1** result in a small intermolecular antiferromagnetic interaction ($J = -0.09 \text{ cm}^{-1}$). The intramolecular exchange coupling in the dinuclear complex **2** is antiferromagnetic ($J = -2.5 \text{ cm}^{-1}$). This antiferromagnetic interaction was analyzed in view of the molecular structure considering spin-polarization, superexchange and orbital-orthogonality. A spin-polarization pathway seems to be the leading contribution which does not involve the 1,3 bridging pathway.

(© Wiley-VCH Verlag GmbH & Co. KGaA, 69451 Weinheim, Germany, 2004)

Introduction

The rational design of polynuclear complexes with ferromagnetic interactions between the paramagnetic centers is central to the development of new classes of molecule-based magnets.^[1] One strategy for synthesizing materials with ferromagnetic interactions is provided by the *meta*-phenylene linkage of organic radicals and carbenes utilizing the spin-polarization mechanism.^[2] This concept has been applied to binuclear transition metal complexes bridged in a *meta*-phenylene arrangement using a variety of bridging ligands.^[3] Some of these compounds do indeed exhibit ferromagnetic interactions between the transition metal ions.^[4–7] However, many complexes with the same kinds of bridging ligands exhibit antiferromagnetic interactions between the transition metal ions.^[8] Several theoretical investigations have been performed in order to obtain an insight into the question of why the concept of spin-polarization cannot be

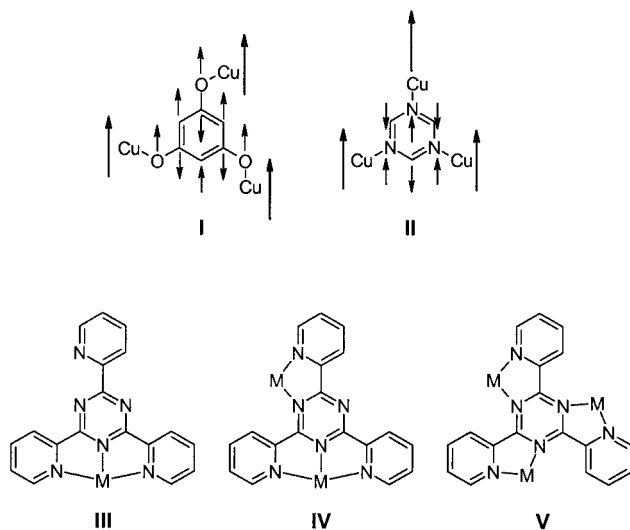
applied in a straightforward manner to transition metal complexes. Bencini et al. showed on resorcinol- and hydroquinone-bridged dinuclear Mo^{V} complexes that for both bridging units not only is the spin-polarization mechanism active but also the superexchange interaction.^[9] The orientation of the magnetic orbital on each metal site relative to the plane of the bridging benzene ring was found to be crucial for a ferromagnetic or an antiferromagnetic contribution of the superexchange interaction as well as of the spin-polarization mechanism. Takano et al. investigated dinuclear Cu^{II} and Mn^{II} complexes with a bridging pyrimidine ligand using DFT and post-Hartree–Fock methods.^[10] They concluded that superexchange interactions leading to antiferromagnetic interactions are more important in *meta*-phenylene bridged transition metal complexes compared with *meta*-phenylene bridged organic carbenes and radicals. Finally, ferromagnetic interactions were proposed in pyrimidine-bridged dinuclear Cu^{II} complexes when the pyrimidine-nitrogen donor of one Cu^{II} center is coordinated equatorially and the pyrimidine-nitrogen donor of the other Cu^{II} center is coordinated axially. Antiferromagnetic interactions were proposed when both nitrogen atoms are coordinated equatorially.^[8a,11]

Recently, we reported the use of modified 1,3,5-trihydroxybenzene (phloroglucinol) ligands to bridge three

^[a] Institut für Anorganische und Analytische Chemie, Westfälische Wilhelms-Universität Münster
Wilhelm-Klemm-Str. 8, 48149 Münster, Germany
Fax: (internat.) +49-251-833-3108
E-mail: tglaser@uni-muenster.de

^[b] Organisch-Chemisches Institut, Westfälische Wilhelms-Universität Münster
Corrensstr. 40, 48149 Münster, Germany

Cu^{II} ions in a *meta*-phenylene linkage.^[12] These complexes exhibit ferromagnetic interactions between the three $S_i = 1/2$ sites to result in a $S_t = 3/2$ spin ground state due to the spin-polarization mechanism (**I** in Scheme 1). In an extended version of these ligands, we incorporated salen-like coordination environments because salen-like ligands form stable complexes with most metal ions.^[13] Just as phloroglucinol is the triangularly topological extension of resorcinol, the triangularly topological extension of pyrimidine is 1,3,5-triazine. We wanted to investigate whether modified 1,3,5-triazine-ligands may be used for the synthesis of trinuclear transition metal complexes with ferromagnetic interactions between the paramagnetic centers based on the spin-polarization mechanism (**II** in Scheme 1).



Scheme 1

Hendrickson and co-workers reported a series of trinuclear Ti^{III} complexes using the tri-anions of cyanuric acid and trithiocyanuric acid as bridging ligands.^[14] While the Ti^{III} centers in the cyanuric bridged complex are antiferromagnetically coupled, a ferromagnetically coupled system was found in the trithiocyanuric system. Recently, Dunbar and co-workers used 1,3,5-triazine-2,4,6-tricarboxylic acid for the synthesis of a one-dimensional chain compound with Fe^{II} ions. However, no exchange interactions between the Fe^{II} centers were observed and this was attributed to the large distance between the paramagnetic centers in the chain. The ferrous ions are not bridged by coordination to one 1,3,5-triazine ring. The ligand bridges the Fe^{II} ions by use of one 1,3,5-triazine nitrogen donor at one site and by a carboxylic group at the other site.^[15] Gamez, Reedijk and co-workers reported an interesting copper coordination polymer using 2,4,6-tris(dipyridin-2-ylamino)-1,3,5-triazine which demonstrated the use of modified 1,3,5-triazine ligands for the construction of higher-dimensional assemblies.^[16]

The modified 1,3,5-triazine ligand 2,4,6-tris(2-pyridyl)-1,3,5-triazine (tptz)^[17] has been used in the spectrophotometric determination of transition metal ions^[18] and as a solvent extraction reagent.^[19] Several transition-metal com-

plexes using the ligand tptz have been reported.^[20–22] The predominant coordination mode of tptz is tri-dentate terpyridine-like (**III** in Scheme 1). However, tptz is also capable of bridging two metal centers in one terpyridine- and one bipyridine-like coordination mode (**IV** in Scheme 1) but no magnetic properties were reported. Several reports have described that coordination of one metal ion, especially Cu^{II}, to tptz induces the hydrolysis of tptz to form bis(2-pyridyl-carbonyl)amine and its complexes.^[22,23]

In order to use tptz as a ferromagnetic coupler between three transition metal ions we investigated whether complexes with tptz as a bridging ligand between three metal ions in bipyridine-like sites would be accessible (**V** in Scheme 1). Herein we report the reaction of tptz with an excess of Cu^{II} ions. In the presence of *N,N*-bis(3-aminopropyl)methylamine (Medpt), only the mononuclear complex [(tptz)Cu^{II}(Medpt)](BF₄)₂·2MeOH (**1**) was isolated. In contrast, reaction of tptz with an excess of CuCl₂·2H₂O resulted in the dinuclear complex [{Cu^{II}Cl₂} (tptz){Cu^{II}Cl₂(MeOH)}] (**2**). No indications of hydrolysis of tptz were observed. Both complexes were fully characterized by single-crystal X-ray diffraction studies and magnetic measurements. To the best of our knowledge complex **2** is the first dinuclear copper complex of tptz and this is the first determination of exchange interactions mediated by the tptz ligand.

Results and Discussion

Synthesis and Spectroscopy

In order to synthesize a trinuclear Cu^{II} complex of type **V** (Scheme 1) with three bipyridine-like coordination sites, additional ligands for complexation of the Cu^{II} centers have to be provided. Since the preferred coordination number of Cu^{II} ions is five, we used an additional tridentate ligand (Medpt). The reaction of tptz with three equivalents of Cu(BF₄)₂·3H₂O and three equivalents of Medpt in methanol resulted in a blue solution from which green crystals of **1** separated upon diffusion of diethyl ether into the solution. The FTIR spectrum of **1** confirmed the presence of the tptz ligand by the absorptions in the 400 to 1600 cm^{−1} region. Two intense N–H bands at 3173 and 3077 cm^{−1} and C–H bands of aliphatic groups between 2800 and 3000 cm^{−1} demonstrate the presence of the Medpt ligand. Additionally, the typical bands of BF₄[−] show the cationic nature of the complex. The electrospray mass spectrum of **1** exhibits a prominent ion at a mass-to-charge ratio (*m/z*) of 259.9, with mass and isotopic distribution patterns corresponding to [(tptz)Cu(Medpt)]²⁺ (calculated *m/z* of 260.1). The elemental analysis combined with these data are in accordance with the formulation of **1** as [(tptz)Cu^{II}(Medpt)](BF₄)₂·2CH₃OH which was corroborated by an X-ray diffraction study.

The reaction of tptz with 15 equivalents of CuCl₂·2H₂O in MeOH resulted in a green solid. Elemental analysis gave a tptz/Cu/Cl ratio of 1:2:4 corresponding to a dinuclear complex and not the 1:3:6 ratio expected for a trinuclear

complex. Diffusion of methanolic solutions of tptz and an excess of $\text{CuCl}_2 \cdot 2\text{H}_2\text{O}$ yielded green needles suitable for single-crystal X-ray diffraction. The FTIR spectrum of **2** exhibits a broad absorption between 2500 and 3200 cm^{-1} indicating the presence of hydrogen bonded O–H groups. The spectrum shows the main signals of the free tptz ligand which are slightly shifted and in most cases split. Structural characterization by a single-crystal X-ray diffraction study enabled the formulation of **2** as $[\{\text{Cu}^{\text{II}}\text{Cl}_2\}(\text{tptz})\{\text{Cu}^{\text{II}}\text{Cl}_2(\text{MeOH})\}]$.

Crystal Structures

Figure 1a shows the molecular structure of the dication $[(\text{tptz})\text{Cu}^{\text{II}}(\text{Medpt})]^{2+}$ in **1** and the labeling scheme used. The asymmetric unit consists of the dication, two BF_4^- anions and two methanol molecules. Selected interatomic distances and angles are listed in Table 1. The copper ion is coordinated by six nitrogen donors (N1, N4, N5 of tptz; N7, N8, N9 of Medpt). The distance between Cu and the triazine nitrogen donor N1 is 2.15 Å whereas the distances with the two pyridyl nitrogen donors N4 and N5 are long at 2.41 Å and 2.50 Å, respectively. The central tertiary amine donor N9 of Medpt is coordinated trans to the triazine nitrogen donor with a bond length of 2.13 Å whereas the primary amine donors N7 and N8 form short bonds of 1.99 Å and 2.00 Å, respectively. The coordination environment of the Cu^{II} ion is best described as an axially elongated octahedron with severe distortion. The equatorial plane consists of N1, N7, N8, and N9 and is orientated perpendicular to the 1,3,5-triazine plane. The angle of 142° sub-

Table 1. Selected bond lengths [Å] and angles [$^\circ$] for **1**

Cu–N1	2.151(2)
Cu–N4	2.414(2)
Cu–N5	2.496(3)
Cu–N7	1.993(2)
Cu–N8	1.995(2)
Cu–N9	2.129(2)
N1–Cu–N4	72.37(6)
N1–Cu–N5	70.37(6)
N1–Cu–N7	86.88(7)
N1–Cu–N8	90.19(7)
N1–Cu–N9	174.20(6)
N4–Cu–N5	142.44(5)
N4–Cu–N7	97.59(7)
N4–Cu–N8	92.57(7)
N4–Cu–N9	102.37(6)
N5–Cu–N7	85.97(7)
N5–Cu–N8	83.02(7)
N5–Cu–N9	115.05(6)
N7–Cu–N8	168.03(8)
N7–Cu–N9	91.48(7)
N8–Cu–N9	92.52(7)

tended by the two axial donors N4 and N5 and the copper center deviates strongly from the ideal N–Cu–N angle of 180° . However, this decreased angle is typical for a Cu^{II} ion in a terpyridine-like environment with the two pyridyl donors in axial positions.

The two di-cations are organized in pairs as “dimers” held together by hydrogen bonds with the methanol solvate molecules (Figure 1b). One methanol forms a hydrogen bond with the uncoordinated pyridyl nitrogen atom (N6–O31' and N6'''–O31'' 2.80 Å). This methanol forms an additional hydrogen bond to a second methanol (O31'–O30'' and O31''–O30' 2.73 Å) while this second methanol forms a hydrogen bond with a coordinated primary amine of a second di-cation (O30''–N7''' and O30'–N7 3.03 Å). The Cu–Cu''' distance is 11.5 Å. However, the shortest Cu–Cu distance in **1** is 7.77 Å. The packing is governed mainly by weak interactions, *viz.* long N–H...F, C–H...F, π – π interactions (there are no strong π – π interactions in **1**) etc.

Figure 2a shows the molecular structure of the dinuclear complex $[\{\text{Cu}^{\text{II}}\text{Cl}_2\}(\text{tptz})\{\text{Cu}^{\text{II}}\text{Cl}_2(\text{MeOH})\}]$ (**2**) and the labeling scheme used. Selected interatomic distances and angles are listed in Table 2. Cu1 is coordinated by tptz in a terpyridine-like coordination mode (**III** in Scheme 1) with two additional chloride donors resulting in five-fold coordination. The Cu1–N1 distance of the triazine nitrogen donor is 1.94 Å and the distances with the two pyridyl donors N26 and N66 of tztz are both 2.07 Å. The chloride Cl12 is coordinated trans to the triazine nitrogen donor N1 at a distance of 2.22 Å whereas chloride Cl11 forms a long bond of 2.51 Å. The coordination geometry of Cu1 may best be described as distorted square pyramidal with N1, N26, N66, and Cl12 forming the equatorial plane and Cl11 occupying the apical position. This equatorial plane is almost coplanar with the 1,3,5-triazine plane. The N26–Cu1–N66 angle of 154° of the terpyridine-like unit is significantly larger compared with the analogous

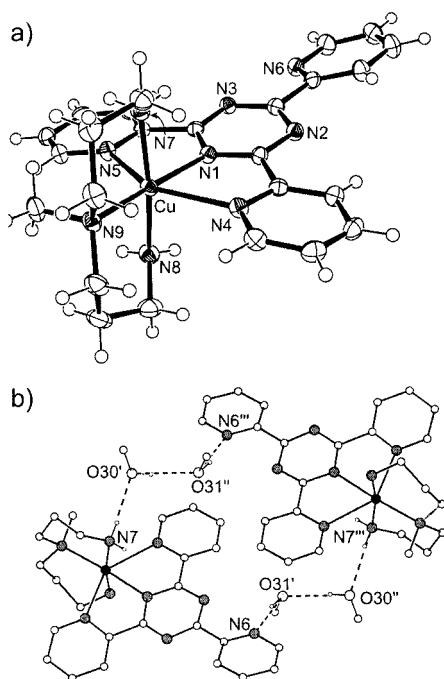


Figure 1. a) Molecular structure of the dication $[(\text{tptz})\text{Cu}^{\text{II}}(\text{Medpt})]^{2+}$ in crystals of **1**. Thermal ellipsoids represent the 50% probability surfaces. b) Schematic view of the “dimeric unit” in **1** formed by hydrogen bonding. [symmetry code: (') $1 - x, 1 - y, 1 - z$; (') $x, y, 1 + z$; (') $1 - x, 1 - y, 2 - z$]

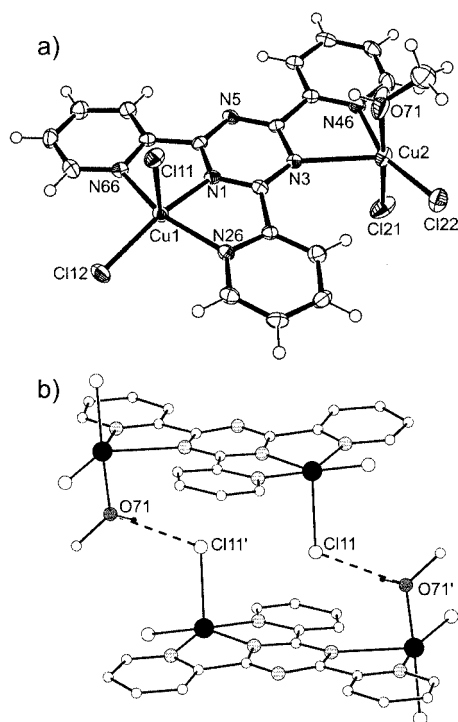


Figure 2. a) Molecular structure of the dinuclear complex $[\{\text{Cu}^{\text{II}}\text{Cl}_2\}(\text{tptz})\{\text{Cu}^{\text{II}}\text{Cl}_2(\text{MeOH})\}]$ in crystals of **2**. Thermal ellipsoids represent the 50% probability surfaces. b) Schematic view of the "dimeric unit" in **2** formed by hydrogen bonding. [symmetry code: (') $2 - x, -y, 2 - z$]

Table 2. Selected bond lengths [Å] and angles [°] for **2**

Cu1–N1	1.942(3)
Cu1–N26	2.072(3)
Cu1–N66	2.073(3)
Cu1–Cl12	2.2192(9)
Cu1–Cl11	2.5093(9)
Cu2–N3	2.454(3)
Cu2–N46	2.023(3)
Cu2–O71	2.045(3)
Cu2–Cl22	2.2220(10)
Cu2–Cl21	2.2391(11)
N1–Cu1–N26	77.60(11)
N1–Cu1–N66	78.45(11)
N1–Cu1–Cl11	98.13(8)
N1–Cu1–Cl12	159.16(8)
N26–Cu1–N66	153.68(10)
N26–Cu1–Cl11	95.02(7)
N26–Cu1–Cl12	100.99(8)
N66–Cu1–Cl11	99.01(8)
N66–Cu1–Cl12	97.50(8)
Cl11–Cu1–Cl12	102.70(4)
N3–Cu2–N46	74.93(10)
N3–Cu2–Cl21	92.63(7)
N3–Cu2–Cl22	123.26(6)
N3–Cu2–O71	85.07(11)
N46–Cu2–Cl21	90.27(8)
N46–Cu2–Cl22	160.40(9)
N46–Cu2–O71	85.54(13)
Cl21–Cu2–Cl22	95.63(4)
Cl21–Cu2–O71	175.63(10)
Cl22–Cu2–O71	88.73(10)

N4–Cu–N5 angle in **1**. This increase originates from the decreased Cu1–N1 bond length of 1.94 Å compared with 2.15 Å in **1** and the different coordination mode of the two pyridyl rings. In **2**, the pyridyl rings are in the equatorial plane (short bonds, 2.07 Å) which is in contrast to **1** where the pyridyl rings occupy axial positions (long bonds, 2.41 and 2.50 Å).

Cu2 is coordinated by tptz in a bipyridine-like coordination mode (**IV** in Scheme 1) with two additional chloride donors and one methanol ligand resulting in a five-fold coordination. The Cu2–N3 bond length of the triazine nitrogen donor at 2.45 Å is the longest found in the two complexes. Conversely, the pyridyl nitrogen donor of tptz N46 forms the shortest pyridyl nitrogen–copper bond at 2.02 Å. Chloride Cl22 is coordinated trans to the pyridyl nitrogen donor at a distance of 2.22 Å and chloride Cl21 is coordinated cis to the pyridyl nitrogen donor at a distance of 2.24 Å. The Cu2–O71 bond length of the coordinated methanol ligand is 2.05 Å. The coordination geometry of Cu2 may also best be described as distorted square pyramidal but in contrast to Cu1 the 1,3,5-triazine nitrogen donor occupies the axial position and the equatorial plane formed by N46, Cl21, Cl22, and O71 is oriented perpendicular to the 1,3,5-triazine plane. With implications for the magnetic properties it is interesting to note that the axial ligand N3 is tilted from a perfect axial position as indicated by the acute N3–Cu2–N46 angle of 75°.

Two molecules of **2** form dimers as a result of two hydrogen bonds which are symmetry related (Figure 2b). The chloride ligand coordinated in the axial position of Cu1 in one molecule forms a hydrogen bond with the coordinated methanol ligand of Cu2 of the other molecule at a distance of 3.01 Å.

Magnetic Properties

The magnetic susceptibilities of **1** and **2** were measured in the temperature range 2–300 K. The raw data were corrected for underlying diamagnetism by using tabulated Pascal's constants and for temperature-independent paramagnetism, χ_{TIP} , which was obtained as a fit parameter. The magnetic properties were analyzed by using the spin Hamiltonian in Equation (1) including the isotropic Heisenberg–Dirac–van Vleck (HDvV) exchange Hamiltonian and the single-ion Zeeman interaction by using a full-matrix diagonalization approach.

$$H = -2J\mathbf{S}_1\mathbf{S}_2 + \sum_i [\mu_B g_i \mathbf{S}_i \mathbf{B}] \quad (1)$$

The effective magnetic moment, μ_{eff} , of complex **1** has a temperature-independent value of 1.84 μ_B in the range 300–30 K and decreases below 30 K to a value of 1.53 μ_B at 2 K (not shown). These data were simulated by using the spin-Hamiltonian for an isolated $S_i = 1/2$ system with $g = 2.123$ and $\chi_{\text{TIP}} = 33 \cdot 10^{-6} \text{ cm}^3 \cdot \text{mol}^{-1}$. However, the decrease below 30 K could not be well reproduced although saturation effects were already taken into account. Thus, the decrease in μ_{eff} reflects intermolecular antiferromagnetic

interactions. We tried to simulate this decrease by introducing a Weiss temperature Θ . The simulation using $\Theta = -0.14$ K resulted in a better agreement, but the simulation was still not satisfactory in the low temperature region. We tried to simulate the magnetic data of **1** using spin Hamiltonian in Equation (1) for a weak exchange coupled dimer. Figure 3 (top) shows the temperature dependence of μ_{eff} calculated for the “dimer **1**”. This model, using the same g -value and χ_{TIP} per site as for the monomeric model described above, gave a satisfactory agreement between experimental and simulated data even in the low temperature range with $J = -0.09$ cm⁻¹. It was not possible to assign the origin of this weak intermolecular antiferromagnetic interaction. Through-space dipolar couplings (closest Cu–Cu distance 7.77 Å) and/or through-bond interactions may account for this weak intermolecular interaction.

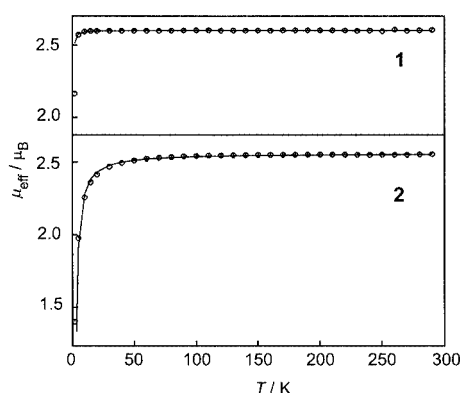
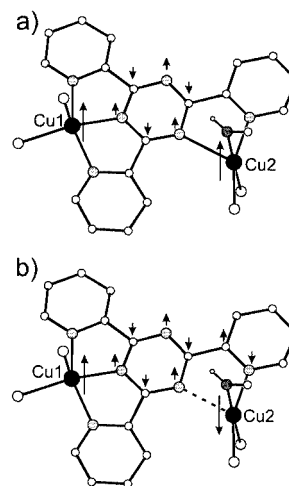


Figure 3. Top: Temperature dependence of the effective magnetic moment, μ_{eff} , calculated for the “dimeric unit” of complex **1** at 1 T. The solid line is a fit of the experimental data using the spin Hamiltonian in Equation (1) with $S_1 = S_2 = 1/2$, $g_1 = g_2 = 2.123$, $\chi_{\text{TIP}} = 66 \cdot 10^{-6}$ cm³·mol⁻¹ for the “dimer”, and $J = -0.09$ cm⁻¹. Bottom: Temperature dependence of the effective magnetic moment, μ_{eff} , of complex **2** at 1 T. The solid line is a fit of the experimental data using the spin Hamiltonian (1) with $S_1 = S_2 = 1/2$, $g_1 = g_2 = 2.090$, $\chi_{\text{TIP}} = 180 \cdot 10^{-6}$ cm³·mol⁻¹, and $J = -2.5$ cm⁻¹.

The effective magnetic moment, μ_{eff} , of the dinuclear complex **2** has a temperature-independent value of $2.55 \mu_{\text{B}}$ in the range 300–110 K and decreases below 110 K to a value of $1.40 \mu_{\text{B}}$ at 2 K (Figure 3 bottom). This is typical behavior for an antiferromagnetically coupled Cu^{II} dimer. The simulation using the spin Hamiltonian in Equation (1) with $g = 2.090$, $\chi_{\text{TIP}} = 180 \cdot 10^{-6}$ cm³·mol⁻¹, and $J = -2.5$ cm⁻¹ nicely reproduces the experimental data. Thus, there is a sizeable exchange coupling through the tptz ligand which is antiferromagnetic in nature.

To the best of our knowledge, the determination of the exchange coupling in **2** is the first established for the tptz ligand. The antiferromagnetic interaction is, at a first glance, counterintuitive to the spin-polarization mechanism mediated by the *meta*-phenylene arrangement of the two copper centers. The spin-polarization should result in a ferromagnetic coupling as depicted in Scheme 2a. However, a close inspection of the molecular structure of **2** results in

a deeper understanding of the exchange coupling in **2**. The magnetic orbitals $d_{x^2-y^2}$ of square-pyramidal-coordinated Cu^{II} ions are located in the equatorial plane. The equatorial plane of Cu1 is orientated parallel to the 1,3,5-triazine ring consisting of N1, N26, N66, and Cl12. In contrast, the equatorial plane of Cu2 is oriented perpendicular to the 1,3,5-triazine ring and consists of N46, Cl12, Cl22, and O71. The $d_{x^2-y^2}$ orbital of Cu1 is delocalized to N1 in a σ -type pathway. There is no delocalization of the $d_{x^2-y^2}$ orbital of Cu2 to N3. First, the Cu2–N3 distance of 2.45 Å is too long for significant delocalization and secondly, the $d_{x^2-y^2}$ orbital of Cu2 is of δ -type symmetry with respect to the Cu2–N3 bond. There is however a strong delocalization of the $d_{x^2-y^2}$ of Cu2 to N46 (Cu2–N46 2.02 Å) in a σ -type pathway. Thus, the spin-polarization mechanism is not operative through the pathway depicted in Scheme 2a but it is operative through a pathway incorporating the pyridyl ring of N46. This pathway for the spin-polarization leads to an antiferromagnetic coupling between the two copper centers (Scheme 2b) and is consistent with the experimental data. The ability of polypyridyl type bridging ligands to mediate spin-polarization over long distances of a ferro- and antiferromagnetic nature depending on the relative arrangement of the pyridyl rings has been demonstrated by McCleverty, Ward, and co-workers.^[3,7]



Scheme 2

As indicated in the introduction, not only the spin-polarization contribution to the exchange coupling but also the superexchange contribution seems to be effective. The orientation of the equatorial planes of the two copper centers is orthogonal. Thus, the magnetic orbitals of Cu1 and Cu2 are orthogonal to each other. This orbital orthogonality was used to understand the ferromagnetic interactions observed in pyrimidine bridged dinuclear Cu^{II} complexes with an equatorial-axial ligation of the pyrimidine bridging ligand.^[8a,11] However, the deviation of the axial triazine nitrogen donor N3 of Cu2 from perfect axial ligation (vide supra) removes the strict orthogonality of the magnetic orbitals and some positive overlap of the $d_{x^2-y^2}$ orbital of Cu2 with the p -orbitals of N3 might occur. Due

to the long bond length, this overlap is weak and gives a small further contribution to the observed antiferromagnetic exchange interaction.

Experimental Section

General Methods and Materials: Infrared spectra (400–4000 cm^{-1}) of solid samples were recorded on a Bruker Vector 22 spectrometer as KBr disks. ESI mass spectra were recorded on a Micromass Quattro LC mass spectrometer. All starting materials were obtained commercially and used without further purification. Temperature-dependent magnetic susceptibilities of finely ground crystals were measured using a SQUID magnetometer (Quantum Design) at 1.0 T (2.0–300 K). For calculations of the molar magnetic susceptibility, χ_M , the measured susceptibilities were corrected for the underlying diamagnetism of the sample using tabulated Pascal's constants. The JULIUS routine was used for spin Hamiltonian simulations using a full-matrix diagonalization approach of the data.^[24]

[(tptz)Cu^{II}(Medpt)](BF₄)₂·2MeOH (1): A solution of Medpt (84 mg, 0.57 mmol) in methanol (5 mL) was added dropwise to a green solution of tptz (60 mg, 0.19 mmol) and Cu(BF₄)₂·3H₂O (168 mg, 0.57 mmol) in methanol (15 mL). The resultant blue solution was stirred for 3 hours. Diffusion of diethyl ether into this solution afforded green crystals. Yield: 95 mg (65%). ESI-MS (positive ion mode): $m/z = 260$ [(tptz)Cu(Medpt)]²⁺. IR (KBr): $\tilde{\nu}/\text{cm}^{-1} = 3315 \text{ w}, 3173 \text{ m}, 3077 \text{ m}, 2956 \text{ w}, 2883 \text{ w}, 2081 \text{ w}, 1660 \text{ m}, 1590 \text{ w}, 1562 \text{ w}, 1522 \text{ m}, 1523 \text{ s}, 1486 \text{ w}, 1470 \text{ w}, 1434 \text{ w}, 1401 \text{ w}, 1385 \text{ s}, 1377 \text{ s}, 1294 \text{ w}, 1264 \text{ m}, 1215 \text{ w}, 1181 \text{ w}, 1084 \text{ s}, 1032 \text{ s}, 1001 \text{ w}, 929 \text{ w}, 862 \text{ w}, 763 \text{ s}, 738 \text{ w}, 675 \text{ m}, 667 \text{ m}, 628 \text{ w}, 620 \text{ w}, 533 \text{ m}, 522 \text{ m}$; elemental analysis calcd. (%) for [(tptz)Cu^{II}(Medpt)](BF₄)₂·2MeOH C₂₇H₃₉B₂CuF₈N₉O₂ (758.83): calcd. C 42.74, H 5.18, N 16.61; found C 42.40, H 4.88, N 16.59.

[(Cu^{II}Cl₂)(tptz){Cu^{II}Cl₂(MeOH)}] (2): Solid tptz (10 mg, 0.032 mmol) and solid CuCl₂·2H₂O (50 mg, 0.29 mmol) were each placed in one arm of an H-shaped tube. The tube was filled carefully with methanol allowing for diffusion of the two solutions between the two arms. During the course of 7 days, green needles appeared. Yield: 19 mg (97%). IR (KBr): $\tilde{\nu}/\text{cm}^{-1} = 3417 \text{ m}, 3137 \text{ m}, 3093 \text{ m}, 3042 \text{ m}, 1608 \text{ w}, 1578 \text{ s}, 1563 \text{ m}, 1544 \text{ s}, 1494 \text{ m}, 1475 \text{ m}, 1445 \text{ w}, 1408 \text{ m}, 1396 \text{ w}, 1377 \text{ s}, 1308 \text{ w}, 1264 \text{ m}, 1154 \text{ w}, 1097 \text{ w}, 1039 \text{ w}, 1016 \text{ m}, 773 \text{ s}, 687 \text{ m}, 668 \text{ m}, 661 \text{ m}, 641 \text{ w}$; elemental analysis calcd. (%) for [(Cu^{II}Cl₂)(tptz){Cu^{II}Cl₂(MeOH)}] C₁₉H₁₆Cl₄Cu₂N₆O (613.26): calcd. C 37.21, H 2.63, N 13.70; found C 36.88, H 2.65, N 13.50.

X-ray Crystal Structure Analysis of [(tptz)Cu^{II}(Medpt)](BF₄)₂·2MeOH (1): Formula C₂₇H₃₉B₂CuF₈N₉O₂, $M = 758.83 \text{ g}\cdot\text{mol}^{-1}$, green crystal $0.45 \times 0.29 \times 0.12 \text{ mm}$, $a = 11.857(2)$, $b = 12.370(2)$, $c = 13.033(2) \text{ \AA}$, $\alpha = 103.01(1)$, $\beta = 109.01(1)$, $\gamma = 103.13(1)^\circ$, $V = 1664.6(4) \text{ \AA}^3$, $\rho_{\text{calcd.}} = 1.514 \text{ g}\cdot\text{cm}^{-3}$, $\mu = 7.43 \text{ cm}^{-1}$, empirical absorption correction ($0.731 \leq T \leq 0.916$), $Z = 2$, triclinic, space group $P\bar{1}$ (No. 2), $\lambda = 0.71073 \text{ \AA}$, $T = 153 \text{ K}$, ω and ϕ scans, 16469 reflections collected ($\pm h, \pm k, \pm l$), $[(\sin\theta)/\lambda] = 0.65 \text{ \AA}^{-1}$, 7635 independent ($R_{\text{int}} = 0.027$) and 6466 observed reflections [$I \geq 2 \sigma(I)$], 621 refined parameters, $R = 0.040$, $wR^2 = 0.098$, max. residual electron density $0.51 (-0.47) \text{ e}\cdot\text{\AA}^{-3}$, hydrogens calculated and refined as riding atoms.

X-ray Crystal Structure Analysis of [(Cu^{II}Cl₂)(tptz){Cu^{II}Cl₂(MeOH)}] (2): formula C₁₉H₁₆Cl₄Cu₂N₆O, $M = 613.26 \text{ g}\cdot\text{mol}^{-1}$, green crystal $0.60 \times 0.10 \times 0.03 \text{ mm}$, $a = 8.332(1)$, $b = 26.006(1)$,

$c = 10.496(1) \text{ \AA}$, $\beta = 99.09(1)^\circ$, $V = 2245.7(4) \text{ \AA}^3$, $\rho_{\text{calcd.}} = 1.814 \text{ g}\cdot\text{cm}^{-3}$, $\mu = 23.96 \text{ cm}^{-1}$, empirical absorption correction ($0.327 \leq T \leq 0.932$), $Z = 4$, monoclinic, space group $P2_1/c$ (No. 14), $\lambda = 0.71073 \text{ \AA}$, $T = 198 \text{ K}$, ω and ϕ scans, 8930 reflections collected ($\pm h, \pm k, \pm l$), $[(\sin\theta)/\lambda] = 0.66 \text{ \AA}^{-1}$, 5113 independent ($R_{\text{int}} = 0.040$) and 3665 observed reflections [$I \geq 2 \sigma(I)$], 293 refined parameters, $R = 0.043$, $wR^2 = 0.094$, max. residual electron density $0.89 (-0.59) \text{ e}\cdot\text{\AA}^{-3}$, hydrogens calculated and refined as riding atoms.

Data sets were collected with Bruker AXS APEX and Nonius Kappa CCD diffractometers, equipped with rotating anode generators. Programs used: data collection SMART^[25] and COLLECT^[26] data reduction SAINT^[25] and Denzo-SMN^[27] absorption correction SADABS^[25] and SORTAV^[28] structure solution SHELXS-97^[29] structure refinement SHELXL-97.^[30]

CCDC-211262 and -211263 contain the supplementary crystallographic data for this paper. These data can be obtained free of charge at www.ccdc.cam.ac.uk/conts/retrieving.html [or from the Cambridge Crystallographic Data Centre, 12 Union Road, Cambridge CB2 1EZ, UK; Fax: (internat.) + 44-1223-336-033; E-mail: deposit@ccdc.cam.ac.uk].

Acknowledgments

T. G. gratefully acknowledges Professor F. E. Hahn for his generous support. This work was supported by the Fonds der Chemischen Industrie (Liebig-Stipendium for T. G.) and the BMBF (Kooperationsbereich Neue Materialien). Dr. E. Bill (Max-Planck-Institut für Strahlenchemie, Mülheim an der Ruhr) is thanked for the magnetic measurements and for valuable discussions.

- [1] O. Kahn, *Acc. Chem. Res.* **2000**, *33*, 647–657.
- [2] [2a] H. C. Longuet-Higgins, *J. Chem. Phys.* **1950**, *18*, 265–274. [2b] H. M. McConnell, *J. Chem. Phys.* **1963**, *39*, 1910. [2c] H. Iwamura, *Adv. Phys. Org. Chem.* **1990**, *26*, 179–253. [2d] A. Rajca, *Chem. Eur. J.* **2002**, *8*, 4834–4841.
- [3] J. A. McCleverty, M. D. Ward, *Acc. Chem. Res.* **1998**, *31*, 842–851.
- [4] Pyrimidine-bridged complexes: [4a] S.-i. Mitsubori, T. Ishida, T. Nogami, H. Iwamura, *Chem. Lett.* **1994**, 285–288. [4b] F. Lloret, G. De Munno, M. Julve, J. Cano, R. Ruiz, A. Caneschi, *Angew. Chem.* **1998**, *110*, 143–145; *Angew. Chem. Int. Ed.* **1998**, *37*, 135–138. [4c] T. Ishida, K. Nakayama, M. Nakagawa, W. Sato, Y. Ishikawa, M. Yasui, F. Iwasaki, T. Nogami, *Synth. Met.* **1997**, *85*, 1655–1658. [4d] T. Ishida, S.-i. Mitsubori, T. Nogami, N. Takeda, M. Ishikawa, H. Iwamura, *Inorg. Chem.* **2001**, *40*, 7059–7064.
- [5] Resorcinol-bridged complexes: [5a] V. Â. Ung, A. M. W. Cargill Thompson, D. A. Bardwell, D. Gatteschi, J. C. McCleverty, F. Totti, M. D. Ward, *Inorg. Chem.* **1997**, *36*, 3447–3454. [5b] V. Â. Ung, S. M. Couchman, J. C. Jeffery, J. A. McCleverty, M. D. Ward, F. Totti, D. Gatteschi, *Inorg. Chem.* **1999**, *38*, 365–369. [5c] H. Oshio, H. Ichida, *J. Phys. Chem.* **1995**, *99*, 3294–3302.
- [6] 1,3-Diaminophenylene-bridged complex: I. Fernández, J. Faus, M. Julve, F. Lloret, J. Cano, X. Ottenwälder, Y. Journeaux, M. C. Muñoz, *Angew. Chem.* **2001**, *113*, 3129–3132; *Angew. Chem. Int. Ed.* **2001**, *40*, 3039–3042.
- [7] Extended Polypyridyl-bridged complexes: A. M. W. Cargill Thompson, D. Gatteschi, J. A. McCleverty, J. A. Navas, E. Rentschler, M. D. Ward, *Inorg. Chem.* **1996**, *35*, 2701–2703.
- [8] [8a] T. Ishida, T. Kawakami, S.-i. Mitsubori, T. Nogami, K. Yamaguchi, H. Iwamura, *J. Chem. Soc., Dalton Trans.* **2002**, 3177–3186. [8b] K. Nakayama, T. Ishida, R. Takayama, D. Hashizume, M. Yasui, F. Iwasaki, T. Nogami, *Chem. Lett.*

- 1998, 497–498. ^[8c] R. Feyderherm, S. Abens, D. Günther, T. Ishida, M. Meißner, M. Meschke, T. Nogami, M. Steiner, *J. Phys.: Condens. Matter* **2000**, *12*, 8495–8509. ^[8d] J. Omata, T. Ishida, D. Hashizume, F. Iwasaki, T. Nogami, *Inorg. Chem.* **2001**, *40*, 3954–3958. ^[8e] T. Kusaka, T. Ishida, D. Hashizume, F. Iwasaki, T. Nogami, *Chem. Lett.* **2000**, 1146–1147. ^[8f] D. R. Corbin, L. B. Francesconi, D. H. Hendrickson, G. D. Stucky, *Inorg. Chem.* **1981**, *20*, 2084–2089.
- ^[9] A. Bencini, D. Gatteschi, F. Totti, D. N. Sanz, J. A. McCleverty, M. D. Ward, *J. Phys. Chem. A* **1998**, *102*, 10545–10551.
- ^[10] Y. Takano, T. Onishi, Y. Kitagawa, T. Soda, Y. Yoshioky, K. Yamaguchi, *Int. J. Quant. Chem.* **2000**, *80*, 681–691.
- ^[11] ^[11a] M. Yasui, Y. Ishikawa, N. Akiyama, T. Ishida, T. Nogami, F. Iwasaki, *Acta Crystallogr., Sect. B* **2001**, *57*, 288–295. ^[11b] F. Mohri, K. Yoshizawa, T. Yamabe, T. Ishida, T. Nogami, *Mol. Eng.* **1999**, *8*, 357–373.
- ^[12] T. Glaser, M. Gerenkamp, R. Fröhlich, *Angew. Chem.* **2002**, *114*, 3984–3986; *Angew. Chem. Int. Ed.* **2002**, *41*, 3823–3825.
- ^[13] ^[13a] T. Glaser, M. Heidemeier, T. Lügger, *J. Chem. Soc., Dalton Trans.* **2003**, 2381–2383. ^[13b] T. Glaser, M. Heidemeier, E. Bill, unpublished results.
- ^[14] ^[14a] B. F. Fieselmann, D. N. Hendrickson, G. D. Stucky, *Inorg. Chem.* **1978**, *17*, 1841–1848. ^[14b] D. R. Corbin, L. B. Francesconi, D. H. Hendrickson, G. D. Stucky, *Inorg. Chem.* **1979**, *18*, 3069–3074. ^[14c] L. B. Francesconi, D. R. Corbin, D. H. Hendrickson, G. D. Stucky, *Inorg. Chem.* **1979**, *18*, 3074–3080.
- ^[15] R.-R. Galan-Mascaros, J. M. Clemente-Juan, K. R. Dunbar, *J. Chem. Soc., Dalton Trans.* **2002**, 2710–2713.
- ^[16] P. Gamez, P. de Hoog, O. Roubeau, M. Lutz, W. L. Driessen, A. L. Spek, J. Reedijk, *Chem. Commun.* **2002**, 1488–1489.
- ^[17] F. H. Case, E. J. Koft, *J. Am. Chem. Soc.* **1959**, *81*, 905–906.
- ^[18] Fe: ^[18a] P. Collins, H. Diehl, G. F. Smith, *Anal. Chem.* **1959**, *31*, 1862–1867. ^[18b] H. Diehl, E. B. Buchanan Jr, G. F. Smith, *Anal. Chem.* **1960**, *32*, 1117–1119. Ru: ^[18c] W. A. Embry, G. H. Ayres, *Anal. Chem.* **1968**, *40*, 1499–1501. Co: ^[18d] M. J. Jammohamed, G. H. Ayres, *Anal. Chem.* **1972**, *44*, 2263–2268.
- ^[19] C. Musikas, X. Vitart, J. Y. Pasquiou, R. Hoel, in *Chemical Separations*, Vol. 1, C. J. King, J. D. Navratil (eds), Litarvan Literature, Denver **1986**.
- ^[20] ^[20a] R. S. Vagg, R. N. Warrenner, E. C. Watton, *Aust. J. Chem.* **1967**, *20*, 1841–1857. ^[20b] G. A. Barclay, R. S. Vagg, E. C. Watton, *Aust. J. Chem.* **1969**, *22*, 643–645. ^[20c] R. S. Vagg, R. N. Warrenner, E. C. Watton, *Aust. J. Chem.* **1969**, *22*, 141–152. ^[20d] H. A. Goodwin, R. N. Sylva, R. S. Vagg, E. C. Watton, *Aust. J. Chem.* **1969**, *22*, 1605–1611. ^[20e] G. A. Barclay, R. S. Vagg, E. C. Watton, *Acta Crystallogr., Sect. B* **1977**, *33*, 3487–3491. ^[20f] G. A. Barclay, R. S. Vagg, E. C. Watton, *Acta Crystallogr., Sect. B* **1978**, *34*, 1833–1837. ^[20g] B. N. Figgis, E. S. Kucharski, S. Mitra, B. W. Skelton, A. H. White, *Aust. J. Chem.* **1990**, *43*, 1269–1276.
- ^[21] ^[21a] X. Chen, F. J. Fernia, J. W. Babich, J. A. Zubieta, *Inorg. Chem.* **2001**, *40*, 2769–2777. ^[21b] S. A. Cotton, V. Franckevicius, J. Fawcett, *Polyhedron* **2002**, *21*, 2055–2061. ^[21c] E. Freire, S. Baggio, J. C. Munoz, R. Baggio, *Acta Crystallogr., Sect. C* **2002**, *58*, m221–m224. ^[21d] P. Byers, G. Y. S. Chan, M. G. B. Drew, M. J. Hudson, *Polyhedron* **1996**, *15*, 2845–2849. ^[21e] N. Gupta, N. Grover, G. A. Neyhart, P. Singh, H. H. Thorp, *Inorg. Chem.* **1993**, *32*, 310–316.
- ^[22] ^[22a] A. Canarero, J. M. Amigo, J. Faus, M. Julve, T. Debaeremaeker, *J. Chem. Soc., Dalton Trans.* **1988**, 2033–2039. ^[22b] J. Faus, M. Julve, J. M. Amigo, T. Debaeremaeker, *J. Chem. Soc., Dalton Trans.* **1989**, 1681–1687.
- ^[23] ^[23a] E. I. Lerner, S. J. Lippard, *J. Am. Chem. Soc.* **1976**, *98*, 5397–5398. ^[23b] E. I. Lerner, S. J. Lippard, *Inorg. Chem.* **1977**, *16*, 1546–1551. ^[23c] T. Kajiwara, A. Kamiyama, T. Ito, *Chem. Commun.* **2002**, 1256–1257. ^[23d] A. Kamiyama, T. Noguchi, T. Kajiwara, T. Ito, *Inorg. Chem.* **2002**, *41*, 507–512. ^[23e] P. Paul, B. Tyagi, M. M. Bhadbhade, E. Suresh, *J. Chem. Soc., Dalton Trans.* **1997**, 2273–2277.
- ^[24] C. Krebs, E. Bill, F. Birkelbach, V. Stämmeler, unpublished results.
- ^[25] SMART, Bruker AXS, **2000**.
- ^[26] Nonius B. V., **1998**.
- ^[27] Z. Otwinowski, W. Minor, *Methods in Enzymology* **1997**, *276*, 307–326.
- ^[28] ^[28a] R. H. Blessing, *Acta Crystallogr., Sect. A* **1995**, *51*, 33–37. ^[28b] R. H. Blessing, *J. Appl. Cryst.* **1997**, *30*, 421–426.
- ^[29] G. M. Sheldrick, *Acta Crystallogr., Sect. A* **1990**, *46*, 467–473.
- ^[30] SHELXL-97, G. M. Sheldrick, Universität Göttingen, **1997**.

Received July 8, 2003

Early View Article

Published Online November 19, 2003